Eur Spine J (2013) 22:1300–1311
DOI 10.1007/s00586-013-2728-2

ORIGINAL ARTICLE

Microarray expression profiling identifies genes with altered expression in Adolescent Idiopathic Scoliosis

Khaled Fendri · Shunmoogum A. Patten · Gabriel N. Kaufman · Charlotte Zaouter · Stefan Parent · Guy Grimard · Patrick Edery · Florina Moldovan

Received: 14 May 2012 / Revised: 14 February 2013 / Accepted: 20 February 2013 / Published online: 7 March 2013

Abstract
Purpose Adolescent Idiopathic Scoliosis (AIS) is considered a complex genetic disease, in which malfunctioning or dysregulation of one or more genes has been proposed to be responsible for the expressed phenotype. However, to date, no disease causing genes has been identified and the pathogenesis of AIS remains unknown. The aim of this study is, therefore, to identify specific molecules with differing expression patterns in AIS compared to healthy individuals.
Methods Microarray analysis and quantitative RT-PCR have examined differences in the gene transcription profile between primary osteoblasts derived from spinal vertebrae of AIS patients and those of healthy individuals.
Results There are 145 genes differentially expressed in AIS osteoblasts. A drastic and significant change has been noted particularly in the expression levels of Homeobox genes (HOXB8, HOXB7, HOXA13, HOXA10), ZIC2, FAM101A, COMP and PITX1 in AIS compared to controls. Clustering analysis revealed the interaction of these genes in biological pathways crucial for bone development, in particular in the differentiation of skeletal elements and structural integrity of the vertebrae.
Conclusions This study reports on the expression of molecules that have not been described previously in AIS. We also provide for the first time gene interaction pathways in AIS pathogenesis. These genes are involved in various bone regulatory and developmental pathways and many of them can be grouped into clusters to participate in a particular biological pathway. Further studies can be built on our findings to further elucidate the association between different biological pathways and the pathogenesis of AIS.

Keywords Adolescent idiopathic scoliosis · Gene expression · Microarray · Bone development

K. Fendri · S. A. Patten · G. N. Kaufman · C. Zaouter · S. Parent · G. Grimard · F. Moldovan (✉)
Sainte-Justine Hospital Research Center,
3175, Chemin de la Cote Ste-Catherine, Montreal,
Quebec H3T 1C5, Canada
e-mail: florina.moldovan@umontreal.ca

S. A. Patten · F. Moldovan
Faculty of Dentistry, University of Montreal, C.P. 6128,
succursale Centre-ville, Montréal, Québec H3C 3J7, Canada

P. Edery
Cytogenetics Service, Civil Hospice of Lyon, Lyon, France

Introduction

Idiopathic Scoliosis (IS) is characterized by a three-dimensional deformity of the spine and its incidence in the general population ranges from 0.15 to 4 % [1]. Adolescent IS (AIS) accounts for 80 % of IS [2]. The origin and cause of AIS remains unknown to date but there are several proposed etiological hypotheses [3] including melatonin deficiency [4] or signaling defect [5], connective tissue abnormalities [6], asymmetries in the central nervous system [7]. abnormal distribution and interaction between melatonin and calmodulin [5, 8] hormonal variation [9], diet, and posture. In addition, there is strong evidence of genetic predisposition to AIS. For instance, familial occurrences of AIS have been reported by many research groups, and concordance for this condition in twins' studies further strengthens the genetic influence on the etiology of AIS. However, controversy exists as to whether the mode of inheritance is multifactorial trait an autosomal dominant trait, or even an X-linked dominant trait. AIS is considered

as a complex genetic disease, in which one or more genes may be responsible for the expressed phenotype, and in which several modifying effects, such as age, sex, and environment, may play specific roles in the phenotypic variation between affected individuals; it is most likely premature to assign responsibility to a single gene.

Recently, chromosomal regions on 6, 10 and 18q [10], 17p11.2, 19p13.3, Xq23–26.1, 8q11, 9q31.2–q34.2, 17q25.3–qtel, 12p13.31 and recently 3q12.1 and 5q13.3 [11] have been associated with AIS. Even genome-wide association studies (GWAS) have recently been used to study genetic predisposition for AIS and although polymorphisms associated with AIS have been described in *SNTG1* on 8q11.22, *ESR1* on 6q25.1, *MATN1* on 1p35, *CHD7* on 8q12.1, *MTNR1B* on 11q21–q22 and *CHL1* [12], no specific genes or proteins have been identified as players in the development of scoliosis. Therefore to gain an insight into the pathogenesis of AIS, we used a microarray approach to study specific alterations in the genetic expression profile of AIS osteoblasts. Our microarray results show that specific subsets of genes are differentially expressed in AIS, which was confirmed for the most part by reverse-transcription-quantitative PCR (RT-qPCR). Furthermore, we observe that the differentially regulated genes could be grouped and assigned to various functional categories, indicating that many regulatory pathways could be involved in AIS pathogenesis.

Materials and methods

Patients

Six unrelated individuals with AIS, and six controls (non-AIS individuals), all French-Canadian females from Quebec were studied. They were examined by the Adam's test and by a standing upright radiograph of the spine. Two independent blinded orthopedic surgeons read the X-rays (clinical features of patients, Table 1). All AIS patients were selected by the same criteria, namely the spinal deformity was a right-thoracic progressive curve requiring corrective spinal surgery. The Cobb angle ranged between 30° and 84°. For the control patients, spinal deformity was excluded by X-ray and clinical examination: they were subjected to spine surgery for traumatic injury. For the experimental design, we choose individuals with the same features for each group to get homogeneous populations. Bone fragments excised during surgery were used to isolate osteoblasts as described below. Each participating subject or, in the case of minors, their legal guardian, gave informed consent. The research protocol was approved by the Research Ethics Committee of Sainte-Justine Hospital.

Primary human osteoblast culture and RNA extraction

Briefly, bone fragments were cultivated in alpha-MEM (supplemented with 10 % (v/v) fetal bovine serum (FBS, Wisent) and 2 mM glutamine, with 100 U/mL penicillin and 100 μg/mL streptomycin (Invitrogen, Burlington, ON, Canada) as antibiotics) at 37 °C. 5 % CO_2 for a period of 28 days, after which the osteoblasts derived from the bone pieces were separated from the remaining bone fragments by trypsinization. To confirm the osteoblasts phenotype, cells were stained for alkaline phosphatase, osteocalcin, osteopontin and collagen type I as we previously described in Letellier et al. [13]. RNA was extracted from osteoblasts using TRIzol Reagent (Invitrogen), according to the manufacturer's instructions, and verification of RNA integrity and concentration were carried out with the Agilent Bioanalyzer 2100 in concert with the Agilent RNA 6,000 nano or pico kit (Agilent) (RNA Quality Testing Services, McGill University and Génome Québec Innovation Centre Montréal Canada).

Microarray gene expression profiling

RNA samples were analyzed using 12 individual Illumina Human HT-12 v3 BeadChip microarrays, which contain probes for 48,804 unique gene expression sequences (from NCBI RefSeq build 38). with 99.99 % coverage specification. Preparatory cDNA synthesis and labeling. microarray hybridization reactions, and data collection were performed according to established protocols at the McGill University and Génome Québec Innovation Centre. Microarray expression data were subsequently analyzed using the FlexArray software (version 1.6.1) a front-end to R and Bioconductor. Probe intensity data were normalized across replicate arrays by robust multi-array average (RMA) and differential gene expression was calculated by empirical Bayes analyses of microarrays (EBAM) with Benjamini-Hochberg false-discovery rate (FDR) correction. Gene expression profiles from primary osteoblasts derived from spinal vertebrae of AIS patients (All AIS with right thoracic curve; $n = 6$) were compared with profiles from the same cells collected from age and sex-matched healthy individuals ($n = 6$). Microarray analysis was conducted on six AIS-Control sample pairs and the data were normalized. To determine those genes that were differentially expressed between AIS cells and control cells, fold-changes between AIS and control cells were calculated. All values were expressed as positive or negative fold changes. Genes that were differentially expressed >1.5-fold, relative to control patient levels, were considered as differentially regulated. Significance analyses of microarrays (SAM) algorithm were then used to calculate FDR-adjusted q-values according to the method of Storey; q-values <0.15 were considered statistically significant.

Table 1 Clinical Features of AIS patients

Patient	Sex	Age at presentation (years)	Location of primary curve	Cobb's angle at diagnosis	Spinal surgery	Bracing	AIS Family history/ethnicity/origin
1	Female	14.97	Right thoracic	30°	Yes	No	Yes/Caucasian/French Canadian
2	Female	12.72	Right thoracic	63°	Yes	Yes	Yes/Caucasian/French Canadian
3	Female	14.74	Right thoracic	32°	Yes	No	No/Caucasian/French Canadian
4	Female	14.46	Right thoracic	78°	Yes	No	Yes/Caucasian/French Canadian
5	Female	13.26	Right-left thoracic	58°–49°	Yes	No	Yes/Caucasian/French Canadian
6	Female	17.78	Right thoracic	84°	Yes	Yes	Yes/Caucasian/French Canadian

Six females with AIS were selected based upon described criteria. The table presents patient characteristics

Functional classification clustering

To compare similarities in gene function in our list of differentially regulated genes, we used the Database for Annotation, Visualization, and Integrated Discovery (DAVID) functional gene clustering algorithm (version 6.7). 145 differentially regulated genes were selected based on our criteria as set forth, and this list was uploaded to the DAVID functional gene clustering web interface. The software compares the uploaded gene list to a gene–gene similarity matrix of over 75,000 functional annotation terms, and generates a cluster map of functionally similar genes using fuzzy heuristic partitioning.

Hierarchical clustering

To reveal potential gene–gene associations in our expression data, we performed hierarchical clustering analysis using Cluster 3.0 software. Briefly, we loaded our list of 145 differentially regulated genes, with the corresponding difference in fold change (as determined above), into the software. We then performed hierarchical clustering calculations using Euclidean distance as a similarity metric, with average linkage as the clustering method. The resulting dendrogram was visualized using Java TreeView (version 1.1.5r2).

Reverse-transcription quantitative PCR

To provide confirmation for our microarray results, the expression levels of a subset of up- and down-regulated genes (in AIS osteoblasts. compared to controls) were evaluated by RT-qPCR analysis. Quantitative PCR was performed for the following genes, selected from the list of genes with the highest fold-changes and those which seem interesting from clustering and functional analysis results. Table 2 displays the primers sequences. Total RNA was prepared from osteoblasts from three AIS patients and from three controls, as described above. Reverse transcription, using poly-deoxythymidine oligos (Invitrogen) as transcription primers, was then performed on 500 ng of RNA that had been treated with ribonuclease-free deoxyribonuclease I (Invitrogen). Quantitative PCR was performed, using SYBR GREEN chemistry as a marker for DNA amplification, on an ABI Prism 7900HT fast real-time PCR system, with 40 cycles of a stepwise amplification (once for 2 min at 50 °C, once for 10 min at 95 °C, 40 times for 15 s at 95 °C, followed by measurement for 1 min at 60 °C). Dissociation curve analysis was performed to ensure product specificity. The fold change of expression was calculated in relation to glyceraldehyde-3-phosphate dehydrogenase (GAPDH) as an internal reference gene, and the expression level was then determined relative to control osteoblasts. Amplification plots, dissociation curves, and threshold cycle (Ct) values were generated by ABI Sequence Detection System software (version 2.4) after data collection, and expression fold-changes were calculated for each gene by the delta–delta Ct method. Individual genes were compared in between AIS patients and controls using Student's t test.

Results

Microarray gene expression

To screen for candidate genes that may contribute to the pathogenesis of AIS, we comparatively analyzed the gene expression patterns of AIS osteoblasts and healthy osteoblasts by microarray analysis. A scatter plot of the microarray data revealed significant gene expression changes in 145 genes in AIS osteoblasts, as compared to controls (Fig. 1; $n = 6$, empirical Bayes, $p < 0.05$). Among these 145 genes, 86 were up-regulated >1.5-fold, such as HOXB8, HOXB7, HOXB5, FLJ30375, ZIC2 and ZIC4 and 59 were down-regulated >1.5-fold, such as HOXA10, HOXA13, HOXA11, FAM101A, TINAGL1, ERAP2, COMP and PITX1. A complete list of up- and down-regulated genes is provided in Table 3.

Table 2 RT-qPCR primers sequences for validated targets

Gene name	Ref_Seq mRNA	Forward primer (5′–3′)	Reverse primer (3′–5′)
HOXB8	NM_024016	GTC CGT GCG CGC CAA TTA TTA	GCC CGT GGT AGA ACT CGT G
HOXB7	NM_004502	CCA GCC TCA AGT TCG GTT TTC	CGC GAA CGC GCT CCA TAG
HOXB5	NM_002147	AAC TCC TTC TCG GGG CGT TAT	CAT CGCATT GTA ATT GTA GCC GT
ZIC2	NM_007129	CAC AAC CAG TAC GGC CGCATG AA	AGC TCC TGC TTG ATG CAC TGC TG
CXCL1	NM_001511	AGG GAA TTC ACC CCA AGA AC	ACT ATG GGG GA T GCA GGA TT
HOXB2	NM_002145	CGT TCC CGA CGT CAA cn CTT	CTC TTC CTC GGA AM AGG GAC
GDF15	NM_004864	CGC GGGACC CTC AGA GTT	CCG CAG CGT GGT TAG CA
DDIT4	NM_019058	AGG AAG CTC ATT GAG TTG TG	GGT ACA TGC TAC ACA CAC AT
SLC7A5	NM_003486	AGA AGG AAG AGG CGC GGG AGA AGA T	AAG ATG CGCGAG CCG ATA ATG GTC
TRIB3	NM_021158	GCC CTG CAC TGC CGTACA G	GGT ACC AGC CAG GAC CTC AGT
CBS	NM_000071	ACA TGC TCT CGT CGC TGC TT	GTG AGG CGG ATC TGT TTG AAC T
PDGFRL	NM_006207	TTG GGT GGA GCT ACC CTG CGT ATC	ACT GGC CGT AGC GCT CAT TCT G
TBX15	NM_152380	ATT CTG GAG ACC TCC TGT GCG C	CCA CAT TGA AAG TGT TGG GGG CC
HCLS1	NM_005335	GAC GGA GAA ACA CGA GTC CCA GAG	TGG TCG GGG CGT CCA TTT CAT TG
PITX1	NM_002653	MG TGG CGTAAG CGC GAG CGT AA	GAC AGC GGG CTC ATG GAG TTG AAG
COMP	NM_000095	TAT CGT TGG TTC CTG CAG CAC CG	GCA TGG TTG TGT CCA AGA CCA CGT
BEX1	NM_018476	CAC TCG TGT CTC GCT ACC AG	CTG CTC GTT TCT CTT TGG ACT C
PCDH10	NM_020815	CAC AAA GTC GAC CAA CAA AA	ATG ATG ACT CCA TCC GAA AT
TGM2	NM_004613	GCC ACT TCA TTT TGC TCT TCA A	TCC TCT TCC GAG TCC AGG TAC A
MAB21L2	NM_011839	CAG CCG CTC AAC AAC TAC CA	CTC GTC CCA GTC CGT TTC TC
BST2	NM_004335	GAT GCA GAG AAG GCC CAA GGA CAA A	ACT TCT TGT CCG CGA TTC TCA CGC
ERAP2	NM_001130140	TGG ATG GGA CCA ACT CAT TAC A	TGC ACC AAC TAG CT AAA CAC
HOXA13	NM_000522	AGC GCG TGC CTT ATA CCA AG	GCC GCT CAG AGA GAT TCG T
HOXA10	NM_018951	AGC CTC GCC GGA GAA GGA TT	CCA GTG TCT GGT GCT TCG TGT AG

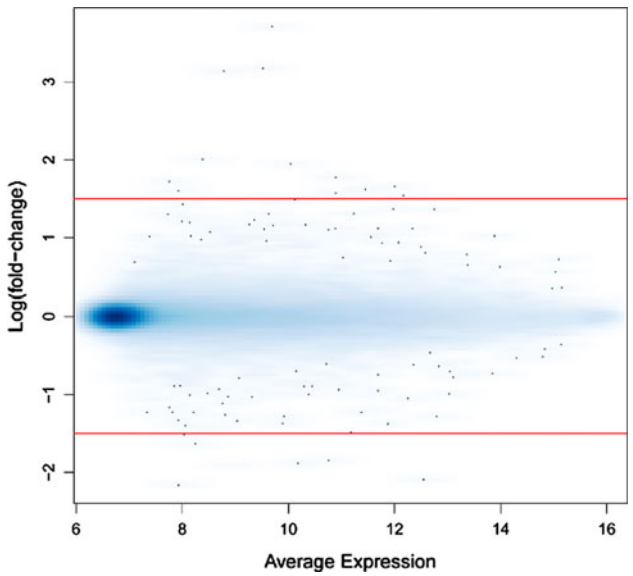

Fig. 1 Scatter plot of microarray gene expression data. Average signal intensity was plotted against the $\log_2$ (fold-change) for all 48.804 probes for the data set of AIS ($n = 6$) minus control ($n = 6$). *Red lines* indicate our threshold of 1.5-fold-change in expression

Functional classification of up-regulated and down-regulated AIS genes

To identify biological pathways common to the differentially expressed genes in AIS osteoblasts, we performed a hierarchical clustering followed by a gene ontology (GO) analysis with DAVID (Database for Annotation, Visualization, and Integrated Discovery) on the 145 differentially expressed genes with a fold change values $\geq$1.5. Interestingly, hierarchical analysis revealed a very close genetic interaction between the down-regulated genes *HOXA13* and *HOXA10* genes, and between *MAB21L2*, *BST2*, *EPYC*, *ERAP2*, *TINAGL1*, *FAM101A* and *HOXA11* genes (Fig. 2). In a second cluster, *EVI2A*, *G0S2*, *HOXB6*, *RASIP1*, *NGEF*. *MYLC2PL* and *HOXA2* genes were found to interact together. Among the up-regulated genes, hierarchical analysis identified one interesting cluster of a closely related genetic interaction between *HOXB8* and *HOXB7*, *HOXB5* and *FLJ30375* and between *ZIC2* and *ZIC4* genes (Fig. 2).

GO analysis of the differentially expressed genes revealed five distinct groups based on similar molecular function and biological process (Group 1–5) (Table 4).

Table 3 Differentially expressed genes

Up-regulated genes				Down-regulated genes			
TargetID	Entrez_gene_ID	$\log_2$ (Fold change)	*P* value	TargetID	Entrez_gene_ID	$\log_2$ (Fold-change)	*P* value
HOXB8	3218	6.35	≤0.001	HOXA10	3206	−5.06	≤0.001
HOXB7	3217	6.25	≤0.001	HOXA13	3209	−3.24	≤0.001
HOXB5	3215	5.32	≤0.001	HOXA11	3207	−2.88	≤0.001
FLJ30375	440982	4.83	≤0.001	FAM101A	144347	−2.87	≤0.001
ZIC2	7546	4.31	≤0.001	TINAGL1	64129	−2.86	≤0.001
ZIC4	84107	4.26	≤0.001	ERAP2	64167	−2.82	≤0.001
HS.347185		3.29	≤0.001	EPYC	1833	−2.82	≤0.001
RERG	85004	2.97	≤0.001	BST2	684	−2.80	≤0.001
HS.539440		2.89	≤0.001	MAB21L2	10586	−2.67	0.01
LOC404266	404266	2.85	≤0.001	LOC130576	130576	−2.48	0.04
HOXB3	3213	2.76	≤0.001	TGM2	7052	−2.33	0.01
HLA-A29.1	649853	2.59	0.03	LRRN3	54674	−2.29	0.01
SMOC2	64094	2.53	0.01	PCDH10	57575	−2.26	0.03
LOC644396	644396	2.51	≤0.001	FMO3	2328	−2.24	0.04
CXCL1	2919	2.51	0.01	BEX1	55859	−2.24	0.02
CHAC1	79094	2.48	0.01	SHOX	6473	−2.23	≤0.001
HOXB2	3212	2.47	≤0.001	GPR116	221395	−2.22	0.01
ZNF608	57507	2.41	≤0.001	COMP	1311	−2.19	0.01
CNTNAP3B	389734	2.38	0.01	FMO3	2328	−2.15	0.06
CXCL2	2920	2.36	0.01	HS.562127		−2.13	0.02
FAM134B	54463	2.30	≤0.001	LYPD6	130574	−2.10	0.01
ADH1A	124	2.28	0.08	TSPAN13	27075	−2.09	0.02
EVI2A	2123	2.18	0.01	RELN	5649	−2.06	≤0.001
G0S2	50486	2.16	0.01	TM4SF20	79853	−2.04	0.01
HOXB6	3216	2.16	≤0.001	EMX2	2018	−2.03	0.01
RASIP1	54922	2.14	≤0.001	PCDH10	57575	−2.01	0.06
NGEF	25791	2.09	0.03	PGF	5228	−1.97	≤0.001
MYLC2PL	93408	2.08	≤0.001	LRRN3	54674	−1.96	0.02
HOXA2	3199	2.06	0.01	FLG	2312	−1.96	0.07
FAM134B	54463	2.03	0.01	LOC284757	284757	−1.93	≤0.001
NOPE	57722	2.02	≤0.001	MYL4	4635	−1.90	≤0.001
HOXA2	3199	2.01	≤0.001	HS.556994		−1.85	≤0.001
HOXD4	3233	1.96	≤0.001	PCDH7	5099	−1.83	0.08
HS.569104		1.96	0.01	F3	2152	−1.82	0.05
FGFBP2	83888	1.91	0.01	PITX1	5307	−1.80	0.05
HS.122310		1.88	0.01	TSPAN13	27075	−1.80	0.02
DDX43	55510	1.87	≤0.001	ACTC1	70	−1.80	0.04
WFDC3	140686	1.87	≤0.001	FAM162B	221303	−1.79	0.08
CX3CL1	6376	1.86	0.02	LOC124220	124220	−1.79	0.01
DENND2A	27147	1.85	0.01	SAMD11	148398	−1.78	≤0.001
XG	7499	1.82	0.03	ECHDC3	79746	−1.77	0.05
AFAP1L2	84632	1.82	≤0.001	S100P	6286	−1.75	0.02
PDGFRL	5157	1.81	0.07	MYPN	84665	−1.74	0.02
PAX9	5083	1.80	≤0.001	TGM2	7052	−1.73	0.03
GDF15	9518	1.77	0.03	LMNB1	4001	−1.71	0.06
DDIT4	54541	1.76	0.03	DLX1	1745	−1.70	≤0.001
MEGF10	84466	1.76	0.02	SPINK5L3	153218	−1.70	0.09

Table 3 continued

Up-regulated genes				Down-regulated genes			
TargetID	Entrez_gene_ID	$\log_2$ (Fold change)	*P* value	TargetID	Entrez_gene_ID	$\log_2$ (Fold-change)	*P* value
SLC7A5	8140	1.75	0.01	HCLS1	3059	−1.69	0.10
FLJ10916	55258	1.74	0.09	CALB2	794	−1.69	≤0.001
TRIB3	57761	1.73	0.03	BARX1	56033	−1.66	0.15
WFDC3	140686	1.70	0.01	TBX15	6913	−1.66	0.01
ZCCHC5	203430	1.70	≤0.001	CDH6	1004	−1.65	0.02
CBS	875	1.68	0.02	MYPN	84665	−1.61	0.01
DCLK1	9201	1.67	≤0.001	TAF13	6884	−1.56	≤0.001
RIMS3	9783	1.67	0.05	EFNB2	1948	−1.54	0.03
EPB41L3	23136	1.66	0.10	ANGPTL7	10218	−1.53	0.03
RPL22L1	200916	1.66	0.03	C2ORF40	84417	−1.52	0.17
NOPE	57722	1.66	0.01	LRRN1	57633	−1.52	0.04
ULBP1	80329	1.66	0.02	NPAS1	4861	−1.51	≤0.001
CH25H	9023	1.65	0.07				
ZBTB46	140685	1.65	≤0.001				
HMCN1	83872	1.65	0.01				
HEY2	23493	1.65	0.09				
F2RL2	2151	1.65	0.02				
SHISA2	387914	1.65	0.01				
SLC7A11	23657	1.64	0.05				
PPL	5493	1.63	0.04				
HOXD1	3231	1.63	0.02				
LSP1	4046	1.62	0.02				
HOXB4	3214	1.61	≤0.001				
REM1	28954	1.61	0.05				
AGTR1	185	1.60	0.02				
KCNG1	3755	1.60	0.01				
PSAT1	29968	1.59	0.02				
LOC285216	285216	1.58	0.01				
IGFBP1	3484	1.58	0.02				
PRPH2	5961	1.54	0.04				
SFRP4	6424	1.54	0.03				
GUCA1B	2979	1.54	0.01				
MAFB	9935	1.53	0.05				
IL18R1	8809	1.53	0.04				
ALG11	440138	1.53	0.01				
SPATA22	84690	1.53	0.15				
MEOX2	4223	1.52	0.01				
CNTN1	1272	1.51	0.10				
AGTR1	185	1.50	0.01				

Genes with a fold-change >1.5 are listed with official NCBI gene symbols, Entrez gene ID numbers, the calculated fold-change, and the associated *p* value calculated as described. A positive $\log_2$ (fold-change) means that the gene was up-regulated in AIS osteoblasts, and a negative one means that the gene was down-regulated

Group 1 consists of 20 genes that are all transcription factors involved in organ development and morphogenesis, as well as in processes of segmentation and anterior/posterior pattern specification. Group 2 is composed of four genes involved in immune system development. Group 3 comprises four genes that are involved in cytokine signaling and secretion. Group 4 contains 17 genes. seven of which are involved in cellular signaling processes related

to cell–cell adhesion and calcium ion binding. The remaining ten genes in cluster group four possess homology domains implicated in cell adhesion and membrane transport. Cluster group 5 is composed of four genes, all zinc finger proteins involved in signal transduction interactions and in ion binding.

RT-qPCR validation of gene expression

To confirm the microarray results 24 genes were chosen for RT-qPCR validation. They were selected because they were the highest fold-changed and they appeared in either functional classification or clustering analyses. Similar patterns of gene expression differences were seen for all genes determined to be down-regulated by our microarray analyses (Fig. 3a, b), thereby confirming our conclusions. Some of the up-regulated by our microarray analyses were also confirmed by RT-qPCR experiments, however no significant up-regulation was observed for *HOXB7*, *ZIC2*, *SLC7A5*, *DDIT4*, *TRIB3*, *CBS*, *GDF15* and *CXCL1* (Fig. 3a).

Profiled genes versus previously reported AIS candidate regions

Several genetic linkage and genome-wide association studies have identified chromosomal loci predisposing to AIS. But to date, no genes have been clearly identified as causative in AIS. We therefore sought to identify if there were any significantly differentially regulated genes in AIS osteoblasts within the reported loci. 32 genes were identified as corresponding with previously reported AIS candidate loci (Table 5). Within region 19p13.3 [14], we identified two genes to be up-regulated: *MKNK2* and *CD70*, *HCLS1* and *COL8A1* genes were down-regulated and *F2R*, *F2RL2* and *BHMT2* genes were up-regulated in the chromosomal regions identified by Edery et al. [11]. Within locus 1p35 [15], *TINAGL1* gene was found down-regulated. Finally, in the AIS candidate region 9q31.2–q34.2 [16], *OLFML2A* was up-regulated. However, none of these genes had a significant fold change $\geq$1.5 (Table 3).

Discussion

In the present work, we have used gene expression profiling to identify differentially expressed genes in AIS compared with non-AIS osteoblasts. Our study provides a previously unrecognized list of genes and related potential pathways that merit further investigation, such as identification of variants in these genes, as putative AIS causative genes. These genes were grouped in terms of their

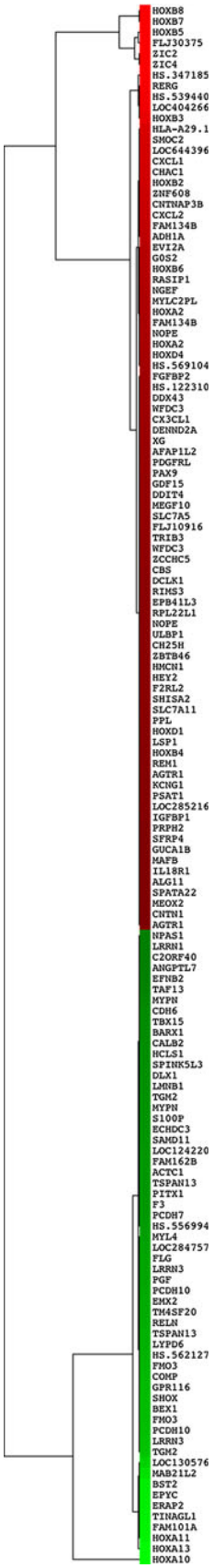

Fig. 2 Hierarchical clustering of gene expression data. The dendrogram provides a measure of relatedness of between the 145 differentially expressed AIS genes. The figure depicts signal strengths for a representative gene. *Colour* indicates relative signal levels, with *red* indicating the highest (up regulated) and *green* indicating the lowest (down regulated) expression

Table 4 Gene interaction networks and gene clusters

official_gene_symbol	Gene name	Entrez_gene_ID	log_2 (Fold-change)
Gene group 1 enrichment score: 8.84			
HOXB8	Homeobox B8	3218	6.35
HOXB7	Homeobox B7	3217	6.25
HOXB5	Homeobox B5	3215	5.32
HOXB3	Homeobox B3	3213	2.76
HOXB2	Homeobox B2	3212	2.47
HOXB6	Homeobox B6	3216	2.16
HOXA2	Homeobox A2	3199	2.06
HOXD4	Homeobox D4	3233	1.96
HOXD1	Homeobox D1	3231	1.63
HOXB4	Homeobox B4	3214	1.61
MEOX2	Mesenchyme homeobox 2	4223	1.52
TBX15	T-box 15	6913	−1.66
BARX1	BARX homeobox 1	56033	−1.66
DLX1	Distal-less homeobox 1	1745	−1.70
PITX1	Paired-like homeodomain 1	5307	−1.80
EMX2	Empty spiracles homeobox 2	2018	−2.03
SHOX	Short stature homeobox	6473	−2.23
HOXA11	Homeobox A11	3207	−2.88
HOXA13	Homeobox A13	3209	−3.24
HOXA10	Homeobox A10	3206	−5.06
Gene group 2 enrichment score: 2.68			
WFDC3	WAP four-disulfide core domain 3	140686	1.87
PDGFRL	Platelet-derived growth factor receptor-like	5157	1.81
ANGPTL7	Angiopoietin-like 7	10218	−1.53
LYPD6	LY6/PLAUR domain containing 6	130574	−2.10
Gene group 3 enrichment score: 2.32			
FGFBP2	Fibroblast growth factor binding protein 2	83888	1.91
GDF15	Growth differentiation factor 15	9518	1.77
SFRP4	Secreted frizzled-related protein 4	6424	1.54
ANGPTL7	Angiopoietin-like 7	10218	−1.53
Gene group 4 enrichment score: 1.20			
CNTNAP3B	Contactin associated protein-like 3B	389734	2.38
FAM134B	FAMILY WITH SEQUENCE SIMILARITY (134 MEMBER B)	54463	2.30
EVI2A	Ecotropic viral integration site 2A	2123	2.18
XG	Xg blood group	7499	1.82
F2RL2	Coagulation factor II (thrombin) receptor-like 2	2151	1.65
SHISA2	Shisa homolog 2 (Xenopus laevis)	387914	1.65
SLC7A11	Solute carrier family 7. member 11	23657	1.64
IL18R1	Interleukin 18 receptor 1	8809	1.53
LRRN1	leucine rich repeat neuronal 1	57633	−1.52
EFNB2	Ephrin-B2	1948	−1.54
CDH6	CADHERIN 6. TYPE 2. K-CADHERIN (FETAL KIDNEY)	1004	−1.65
FAM162B	Family with sequence similarity (162 member B)	221303	−1.79
TSPAN13	TETRASPANIN 13	27075	−1.80
PCDH7	Protocadherins (7)	5099	−1.83
PCDH10	Protocadherins (10)	57575	−2.01
TM4SF20	Transmembrane 4 L six family member 20	79853	−2.04

Table 4 continued

official_gene_symbol	Gene name	Entrez_gene_ID	$\log_2$ (Fold-change)
GPR116	G protein-coupled receptor 116	221395	−2.22
GENE group 5 enrichment score: 0.39			
ZIC4	Zinc finger protein. ZNF of the cerebellum 4	84107	4.26
ZNF608	Zinc finger protein. ZNF608	57507	2.41
ZCCHC5	Zinc finger protein with CCHC domain containing 5	203430	1.70
ZBTB46	Zinc finger protein with BTB domain containing 46	140685	1.65

The 46 genes that were clustered by the DAVID algorithm are listed in their five gene cluster groupings with gene enrichment scores, with associated fold-changes per gene. Gene cluster analysis of differentially regulated genes in primary human osteoblasts. Up-regulated genes are shown in red, Down-regulated genes are shown in green

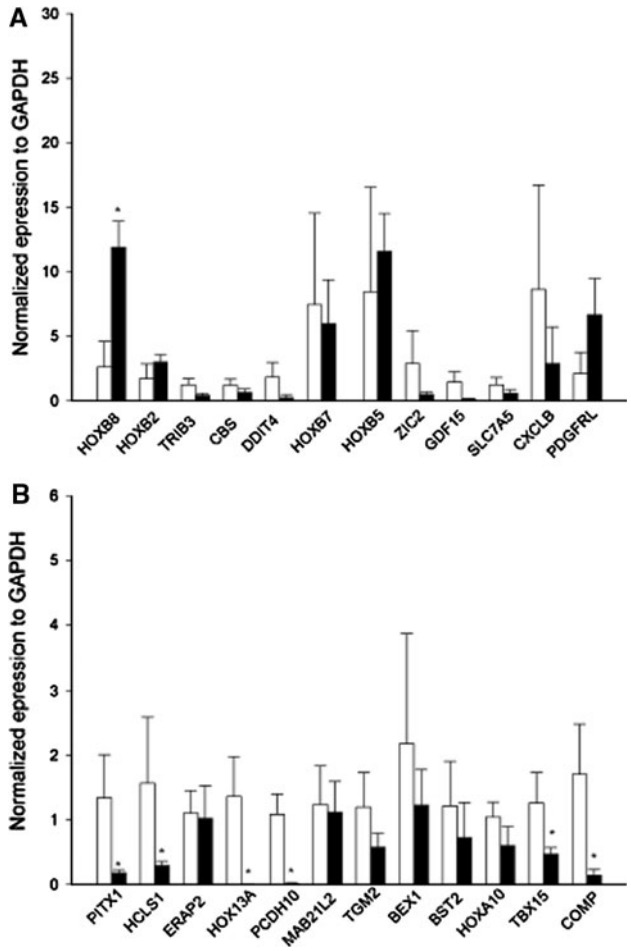

Fig. 3 Validation of most up-regulated (**a**) and down-regulated (**b**) genes by RT-qPCR. The relative level of mRNA of regulated genes was analyzed by quantitative RT-PCR. Gene expression results are depicted as ΔCt values, normalized to GAPDH. $*p < 0.05$, Student's *t* test, AIS (■) versus control (□) expression levels

biological function, and clustered by gene–gene interactions. We identified at least four particular pathways that might be important in AIS: the developmental/growth-differentiation of skeletal elements (*HOXB8*, *HOXA2*, *HOXB2*, *MEOX2* and *PITX1*); cellular signaling (*HOXA11* and *BARX1*), connecting structural integrity of the extracellular matrix to the structural integrity of a bone or a muscle fiber (*COMP*, *HOXA2* and *HOXA11*); and cellular signaling and cartilage damage (*GDF15*). Among the differentially expressed genes, some could act on processes directly related to the causes of AIS (associated with embryogenesis/morphogenesis), while others may play contributory roles (related to spinal deformity progression). Yet others may be condition-specific genes (differentially expressed genes as a consequence of disease).

Our results revealed that the most up- and down-regulated genes involved in the AIS pathology are members of the Homeobox (HOX) gene family. The HOX genes are, in general, implicated in the regulation of patterns of development (morphogenesis). We identified differential expression of HOXA group genes (10, 11 and 13), of HOXB group genes (2–8) and of HOXD (1–4). Interestingly, knockdown of *Hoxd1* generates defects in hindbrain and neural crest derivatives [17]. The over-expression of *Hoxd4* has resulted in severe cartilage defects in mice [18], while over-expression of *Hoxb8* in transgenic mouse embryos has resulted in defects in the vertebrae [19]. *HOXA10* plays a key role in regulating target genes for osteoblast differentiation and bone formation in the postnatal skeleton [20]. *HOXA13* gene is involved particularly in segment identity specification along the limb axis in vertebrates [21]. These suggest that HOX genes are important in vertebral development and abnormal expression of these genes as we observed in AIS patients could play a role in curvation of the spine.

PITX1 (pituitary homeobox 1) gene encodes for a protein that is a member of RIEG/PITX homeobox family with transcriptional properties that have been defined for number of late downstream target genes in the pituitary gland [22]. As a member of this family, *PITX1* gene is involved in limb and organ development and in left–right asymmetry [23]. The down-regulated expression of *PITX1* in our study confirms that this protein plays a crucial role in bone

Table 5 Transcriptome profile of genes within reported AIS candidate loci

Candidate region	References	Candidate gene	Ref_Seq	Chromosomal Localization	Fold-Change
11q21–q22	Qiu et al. [30]	MMP13	NM_002427.2	11q22.2b	0.62
1p35	Montanaro et al. [15]	TINAGL1	NM_022164.1	1p35.2a	−1.05
		IFI6	NM_022872.2	1p35.3b	−0.84
		SESN2	NM_031459.3	1p35.3b	0.76
6q25.1	Wu et al. [31]	ULBP1	NM_025218.2	6q25.1b	0.9
19p13.3	Chan et al. [14]	CD70	NM_001252.3	19p13.3a	0.71
	Alden et al. [32]	MKNK2	NM_017572.2	19p13.3 h	0.93
12p13.31	Raggio et al. [33]	CD4	NM_000616.3	12p13.31d	−0.32
		NTF3	NM_002527.3	12p13.31e	0.89
17q25.3–qtel	Ocaka et al. [16]	ARL16	NM_001040025.1	17q25.3f	−0.27
9q31.2–q34.2	Ocaka et al. [16]	PTGS1	NM_080591.1	9q33.2b	−0.86
		OLFML2A	NM_182487.2	9q33.3a	0.96
Xq23–26.1	Justice et al. [34]	GRIA3	NM_000828.3	Xq25b	−0.56
		GPC4	NM_001448.2	Xq26.2b	0.62
		MGC16121	XM_001128419.1	Xq26.3a	0.68
17p11.2	Salehi et al. [35]	EPPB9	NM_015681.2	17p11.2e	−0.48
		SPECC1	NM_001033554.1	17p11.2d-p11.2c	−0.31
18q	Wise et al. [10]	LOC284293	XM_209104.2	18q21.33b	−0.32
		BCL2	NM_000633.2	18q21.33b	0.48
10q	Wise et al. [10]	DDIT4	NM_019058.2	10q22.1f	1.62
		DKK1	NM_012242.2	10q21.1a	−1.28
		EMX2	NM_004098.2	10q26.11a	−0.89
		SVIL	NM_003174.3	10p11.23b	1.01
6q	Wise et al. [10]	FAM162B	NM_001085480.1	6q22.2a	−0.9
		SMOC2	NM_022138.1	6q27d–q27e	1.03
3q13.3	Edery et al. [11]	COL8A1	NM_001850	3q12.1b–q12.1c	−0.97
		HCLS1	NM_005335.3	3q13.33c	−1.42
5q13	Edery et al. [11]	FOXD1	NM_004472.2	5q13.2c	0.57
		F2R	NM_001992.2	5q13.3d	1.04
		F2RL2	NM_004101.2	5q13.3d	0.97
		BHMT2	NM_017614.3	5q14.1c	0.68

The table presents a list of genes within AIS reported loci and their corresponding fold-changes. As revealed by microarray analysis

development and probably in AIS. Furthermore, Cartilage oligomeric matrix protein (*COMP*) is a novel gene to consider in the context of AIS pathogenesis. This gene is essential for the normal development of cartilage and for its conversion to bone during growth. For instance, *COMP* also interacts with the transcription factor SOX-9, which plays an important role in normal skeletal development. Mutations in *COMP* produce clinical phenotypes of pseudoachondroplasia (PSACH) and multiple epiphyseal dysplasia (MED). These disorders are characterized by disproportionate short stature, brachydactyly, joint hyper-mobility, early-onset osteoarthritis, and scoliosis [24]. Consistent with our study, *COMP* was recently found to be down-regulated by fourfold in AIS compared to unaffected individuals and it was proposed as an important and novel biomarker in predicting scoliosis development [25]. Interestingly, *COMP* and *HOXA10* interact closely in embryonic limb morphogenesis (GO: 0030326. http://amigo.geneontology.org) and with *ERAP2*; which is associated with familial ankylosing spondylitis and it affects joints and can cause eventual fusion of the spine [26]. Altogether, these data suggest that low expression of *COMP* and its molecular interactions are associated with AIS.

Other modulated genes in our experiment include *BST2*, *HCLS1*, *TBX15*, *PCDH10* and *GDF15*. Although these genes are not directly involved in bone and cartilage development, they are involved in immune process and Wnt, tyrosine kinase signaling pathways that are important in the embryonic development and may be associated with AIS.

Our study screened candidate genes that may contribute to the pathogenesis of AIS, and provided a new list of genes that merit further investigation. such as the

epigenetic interactions (that could modify the expression of specific genes) as well as the identification of variants in these genes, as possible AIS contributing genes. We found that the gene expression patterns of primary osteoblasts derived from spinal vertebrae of AIS patients were different from those of healthy individuals. Gene mutations can affect gene transcripts. In addition, the expression of specific genes by cells can be modified by various ways: enzymes methylate DNA to modulate transcription, histone modification resulting in inducing or repression of target sequences, non-coding small RNA which could attach to messengers RNA to modify gene expression of specific genes [27, 28]. Therefore, it is likely that these mechanisms might play an important role in the altered gene expression patterns in AIS osteoblasts. Genes with altered expression in AIS could be grouped into specific subsets based on their biological functions and gene–gene interactions, suggesting the possible involvement of various pathways in AIS pathogenesis. Interestingly, patients with AIS with similar gene profiles may have varying severity of spinal curve suggesting that genetic factors likely control disease susceptibility and course, but not disease pattern. Hormonal and environmental factors may also affect the clinical phenotype and the severity of curve [29] although patients may have the similar gene profiles but this area remains unexplored and beyond the scope of this study.

Taken together our study revealed gene expression changes in AIS osteoblasts. These findings help to gain further insights into potential genes and molecular pathways that could contribute to understanding the pathophysiology of idiopathic scoliosis. Furthermore, although bone contributes significantly in developing AIS, the intervertebral discs (IVD) and muscles also have significant mechanisms in the pathogenesis of AIS. Therefore, our approach can be helpful to study the gene expression profile of AIS IVD and muscles and to further add to our understanding of AIS etiology. Identification of the underlying mechanisms that leads to the observed clinical features of scoliosis remains the crucial next step to further advance understanding of AIS pathogenesis.

Acknowledgments FM and PE were supported by Yves Cotrel Foundation and SAP was supported by CHU Sainte-Justine and Foundation of the Stars scholarship.

Conflict of interest None.

References

1. Je L (1995) Idiopathic Scoliosis. In: Winter RB, Ogilive JW (eds) Lonstein JE BD. Moe's textbook of scoliosis and other spinal deformaties. WB Saunders, Philadelphia, pp 219–256
2. Cavallaro Goodman C, Fuller KS (2009) Pathology: implications for the physical therapist. Saunders. WB/CO, St. Louis
3. Winter RB (1979) Posterior spinal fusion in scoliosis: indications technique and results. Orthop Clin N Am 10:787–800
4. Dubousset JQP, Thillard M (1983) Experimental scoliosis induced by pineal and diencephalic lesions in young chickens: its relation with clinical findings. Orthop Trans 7:7–12
5. Machida M, Dubousset J, Imamura Y, Miyashita Y, Yamada T, Kimura J (1996) Melatonin a possible role in pathogenesis of adolescent idiopathic scoliosis. Spine 21:1147–1152
6. Taylor TK, Ghosh P, Bushell GR (1981) The contribution of the intervertebral disk to the scoliotic deformity. Clin Orthop Relat Res 156:79–90
7. Sahlstrand T, Petruson B (1979) A study of labyrinthine function in patients with adolescent idiopathic scoliosis I. An electro-nystagmographic study. Acta orthop Scand 50:759–769
8. Kindsfater K, Lowe T, Lawellin D, Weinstein D, Akmakjian J (1994) Levels of platelet calmodulin for the prediction of progression and severity of adolescent idiopathic scoliosis. J Bone Jt Surg Am 76:1186–1192
9. Nissinen M, Heliovaara M, Seitsamo J, Poussa M (1993) Trunk asymmetry. posture. growth. and risk of scoliosis. A three-year follow-up of Finnish prepubertal school children. Spine 18:8–13
10. Wise CA, Barnes R, Gillum J, Herring JA, Bowcock AM, Lovett M (2000) Localization of susceptibility to familial idiopathic scoliosis. Spine 25:2372–2380
11. Edery P, Margaritte-Jeannin P, Biot B, Labalme A, Bernard JC, Chastang J, Kassai B, Plais MH, Moldovan F, Clerget-Darpoux F (2011) New disease gene location and high genetic heterogeneity in idiopathic scoliosis. Eur J Hum Genet 19:865–869. doi:10.1038/ejhg.2011.31
12. Sharma S, Gao X, Londono D, Devroy SE, Mauldin KN, Frankel JT, Brandon JM, Zhang D, Li QZ, Dobbs MB, Gurnett CA, Grant SF, Hakonarson H, Dormans JP, Herring JA, Gordon D, Wise CA (2011) Genome-wide association studies of adolescent idiopathic scoliosis suggest candidate susceptibility genes. Hum Mol Genet 20:1456–1466. doi:10.1093/hmg/ddq571
13. Letellier K, Azeddine B, Parent S, Labelle H, Rompre PH, Moreau A, Moldovan F (2008) Estrogen cross-talk with the melatonin signaling pathway in human osteoblasts derived from adolescent idiopathic scoliosis patients. J Pineal Res 45:383–393. doi:10.1111/j.1600-079X.2008.00603.x
14. Chan V, Fong GC, Luk KD, Yip B, Lee MK, Wong MS, Lu DD, Chan TK (2002) A genetic locus for adolescent idiopathic scoliosis linked to chromosome 19p13.3. Am J Hum Genet 71:401–406. doi:10.1086/341607
15. Montanaro L, Parisini P, Greggi T, Di Silvestre M, Campoccia D, Rizzi S, Arciola CR (2006) Evidence of a linkage between matrilin-1 gene (MATN1) and idiopathic scoliosis. Scoliosis 1:21. doi:10.1186/1748-7161-1-21
16. Ocaka L, Zhao C, Reed JA, Ebenezer ND, Brice G, Morley T, Mehta M, O'Dowd J, Weber JL, Hardcastle AJ, Child AH (2008) Assignment of two loci for autosomal dominant adolescent idiopathic scoliosis to chromosomes 9q31.2-q34.2 and 17q25.3-qtel. J Med Genet 45:87–92. doi:10.1136/jmg.2007.051896
17. McNulty CL, Peres JN, Bardine N, van den Akker WM, Durston AJ (2005) Knockdown of the complete Hox paralogous group 1 leads to dramatic hindbrain and neural crest defects. Development 132:2861–2871. doi:10.1242/dev.01872
18. Pollock RA, Sreenath T, Ngo L, Bieberich CJ (1995) Gain of function mutations for paralogous Hox genes: implications for the evolution of Hox gene function. Proc Natl Acad Sci USA 92:4492–4496
19. Yang X, Ji X, Shi X, Cao X (2000) Smad1 domains interacting with Hoxc-8 induce osteoblast differentiation. J Biol Chem 275:1065–1072

20. Riggs BL, Khosla S, Melton LJ 3rd (2002) Sex steroids and the construction and conservation of the adult skeleton. Endocr Rev 23:279–302
21. Mortlock DP, Innis JW (1997) Mutation of HOXA13 in hand-foot-genital syndrome. Nat Genet 15:179–180. doi:10.1038/ng0297-179
22. Logan M, Tabin CJ (1999) Role of Pitx1 upstream of Tbx4 in specification of hindlimb identity. Science 283:1736–1739
23. Gurnett CA, Alaee F, Kruse LM, Desruisseau DM, Hecht JT, Wise CA, Bowcock AM, Dobbs MB (2008) Asymmetric lower-limb malformations in individuals with homeobox PITX1 gene mutation. Am J Hum Genet 83:616–622. doi:10.1016/j.ajhg.2008.10.004
24. Briggs MD, Chapman KL (2002) Pseudoachondroplasia and multiple epiphyseal dysplasia.: mutation review molecular interactions, and genotype to phenotype correlations. Hum Mutat 19:465–478. doi:10.1002/humu.10066
25. Fendri K, Moldovan F (2011) Potential role of COMP as a biomarker for adolescent idiopathic scoliosis. Med Hypotheses 76:762–763. doi:10.1016/j.mehy.2011.01.038
26. Tsui FW, Haroon N, Reveille JD, Rahman P, Chiu B, Tsui HW, Inman RD (2010) Association of an ERAP1 ERAP2 haplotype with familial ankylosing spondylitis. Ann Rheum Dis 69:733–736. doi:10.1136/ard.2008.103804
27. Hamilton JP (2011) Epigenetics: principles and practice. Dig Dis 29:130–135. doi:10.1159/000323874
28. Silahtaroglu A, Stenvang J (2010) MicroRNAs epigenetics and disease. Essays Biochem 48:165–185. doi:10.1042/bse0480165
29. Burwell RG, Dangerfield PH, Moulton A, Grivas TB (2011) Adolescent idiopathic scoliosis (AIS), environment. exposome and epigenetics: a molecular perspective of postnatal normal spinal growth and the etiopathogenesis of AIS with consideration of a network approach and possible implications for medical therapy. Scoliosis 6:26. doi:10.1186/1748-7161-6-26
30. Qiu XS, Tang NL, Yeung HY, Lee KM, Hung VW, Ng BK, Ma SL, Kwok RH, Qin L, Qiu Y, Cheng JC (2007) Melatonin receptor 1B (*MTNR1B*) gene polymorphism is associated with the occurrence of adolescent idiopathic scoliosis. Spine (Phila Pa 1976) 32(16):1748–1753
31. Wu J, Qiu Y, Zhang L, Sun Q, Qiu X, He Y (2006) Association of estrogen receptor gene polymorphisms with susceptibility to adolescent idiopathic scoliosis. Spine (Phila Pa 1976) 31(10):1131–1136
32. Alden KJ, Marosy B, Nzegwu N, Justice CM, Wilson AF, Miller NH (2006) Idiopathic scoliosis: identification of candidate regions on chromosome 19p13. Spine (Phila Pa 1976) 31(16):1815–1819
33. Raggio CL, Giampietro PF, Dobrin S, Zhao C, Dorshorst D, Ghebranious N, Weber JL, Blank RD (2009) A novel locus for adolescent idiopathic scoliosis on chromosome 12p. J Orthop Res 27:1366–1372
34. Justice CM, Miller NH, Marosy B, Zhang J, Wilson AF (2003) Familial idiopathic scoliosis: evidence of an X-linked susceptibility locus. Spine 28:589–594
35. Salehi LB, Mangino M, De Serio S, De Cicco D, Capon F, Semprini S, Pizzuti A, Novelli G, Dallapiccola B (2002) Assignment of a locus for autosomal dominant idiopathic scoliosis (IS) to human chromosome 17p11. Hum Genet 111:401–404